# Comparison of wind turbine wake properties in non-uniform inflow predicted by different CFD rotor models

**Troldborg, Niels; Zahle, Frederik; Sørensen, Niels N.; Réthoré, Pierre-Elouan**

*Publication date:*
2012

# Comparison of wind turbine wake properties in non-uniform inflow predicted by different CFD rotor models

Niels Troldborg, Frederik Zahle, Niels N. Sørensen, Pierre-Elouan Réthoré

Wind Energy Department, DTU Wind Energy, DK-4000 Roskilde, Denmark

Risø DTU
National Laboratory for Sustainable Energy

# Background

| Wind turbine models in CFD |
| --- |
| • Fully resolved rotor (FR) |
| • Actuator line model (AL) |
| • Actuator disc model (AD) |

# Background

**Wind turbine models in CFD**

- Fully resolved rotor (FR)
- Actuator line model (AL)
- Actuator disc model (AD)

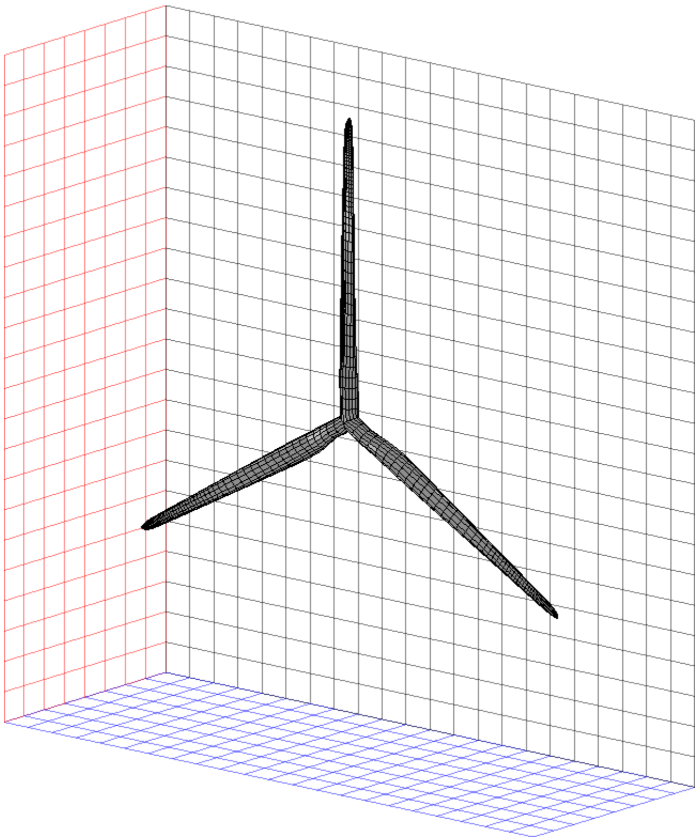

- The blade/airfoil boundary layer is resolved
- The required number of grid points for one rotor using RANS is $O(10^7)$
- Provides detailed insight about flow behaviour
- Usually used for accurately predict loads and power production
- Too computationally heavy for several wind turbines.

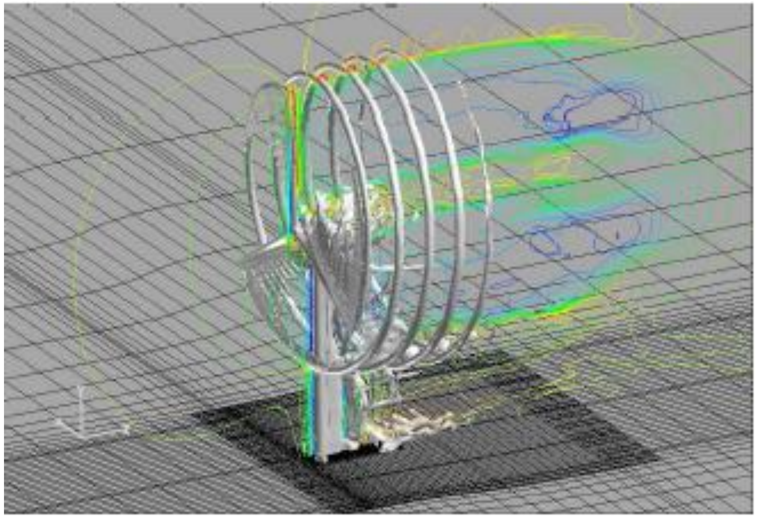

# Background

| Wind turbine models in CFD |
|---|
| • Fully resolved rotor (FR) |
| • Actuator line model (AL) |
| • Actuator disc model (AD) |

➢ Blades represented as lines.

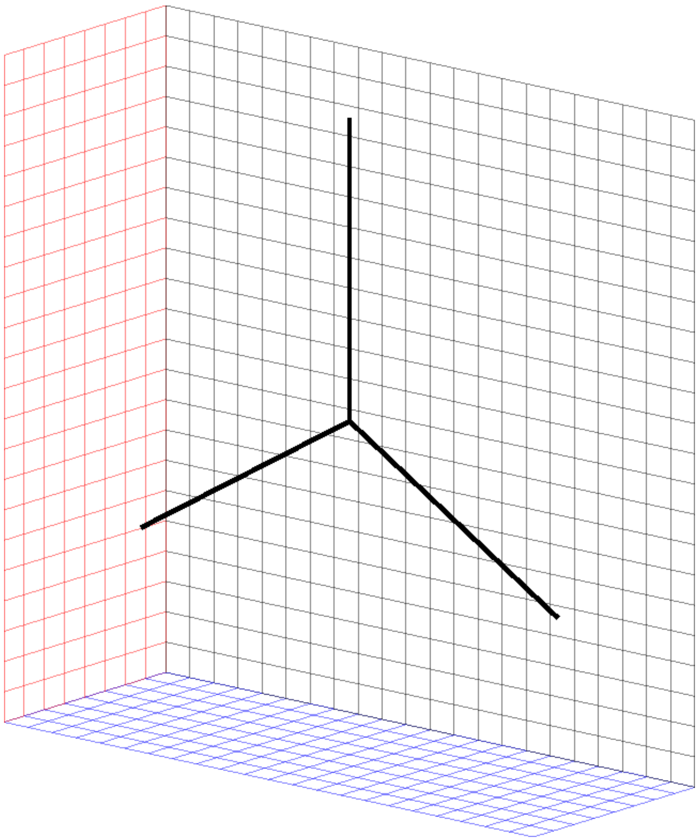

# Background

**Wind turbine models in CFD**

- Fully resolved rotor (FR)
- Actuator line model (AL)
- Actuator disc model (AD)

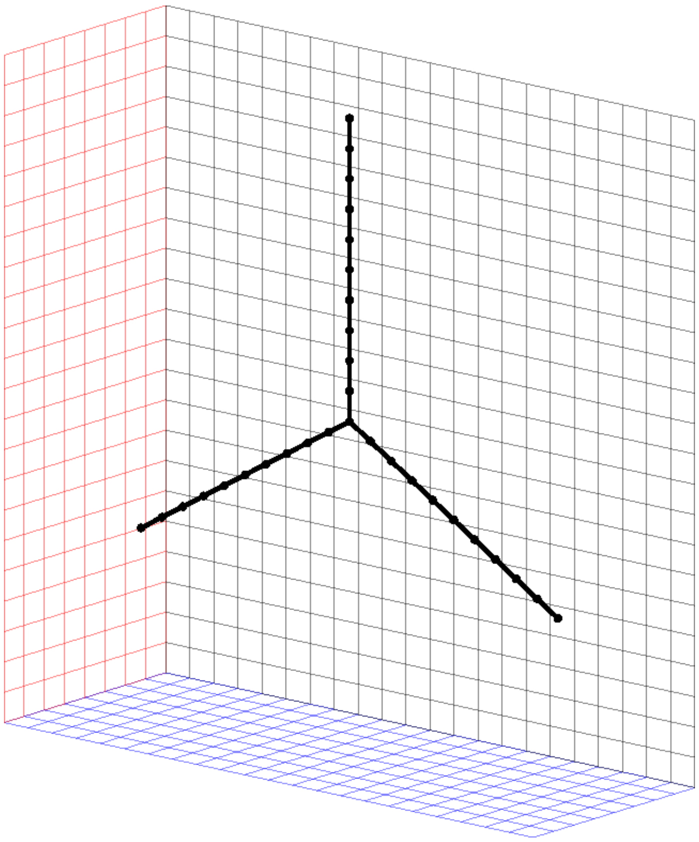

- Blades represented as lines.
- Aerodynamic blade forces determined from 2D airfoil data.

# Background

**Wind turbine models in CFD**

- Fully resolved rotor (FR)
- Actuator line model (AL)
- Actuator disc model (AD)

➢ Blades represented as lines.

➢ Aerodynamic blade forces determined from 2D airfoil data.

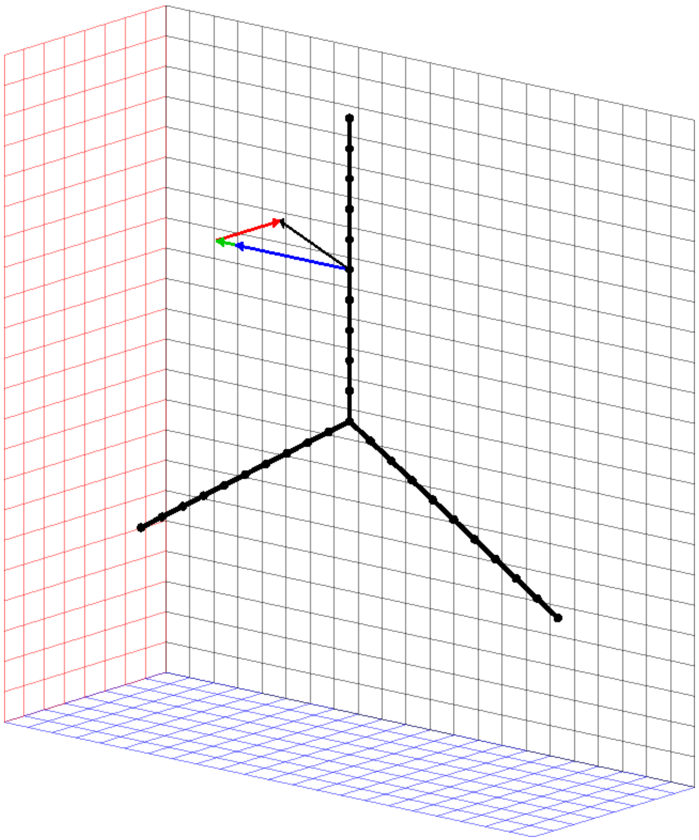

$$\varphi = \tan^{-1}\left(\frac{V_z}{\Omega r - V_\theta}\right)$$
$$\Downarrow$$
$$\alpha = \varphi - \gamma$$

$$\mathbf{f} = \begin{pmatrix} L \\ D \end{pmatrix} = \tfrac{1}{2}\rho V_{rel}^2 c \begin{pmatrix} C_L(\alpha)\mathbf{e}_L \\ C_D(\alpha)\mathbf{e}_D \end{pmatrix}$$

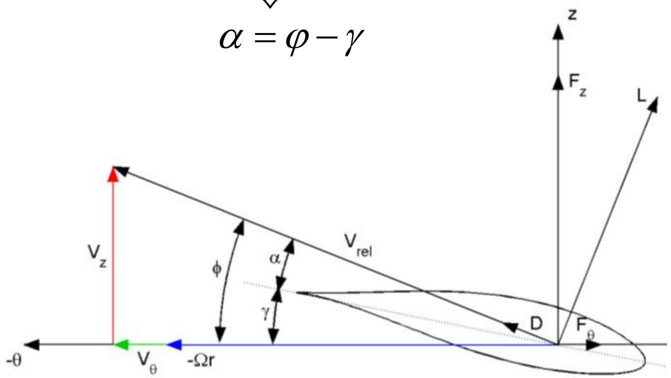


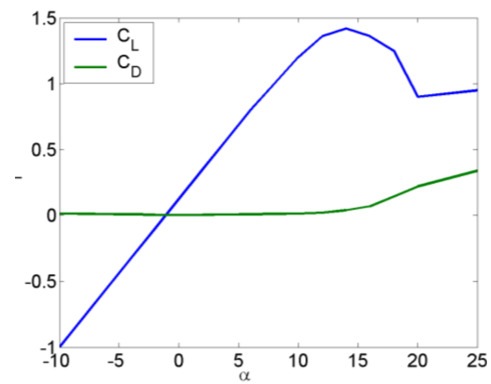

# Background

**Wind turbine models in CFD**

- Fully resolved rotor (FR)
- Actuator line model (AL)
- Actuator disc model (AD)

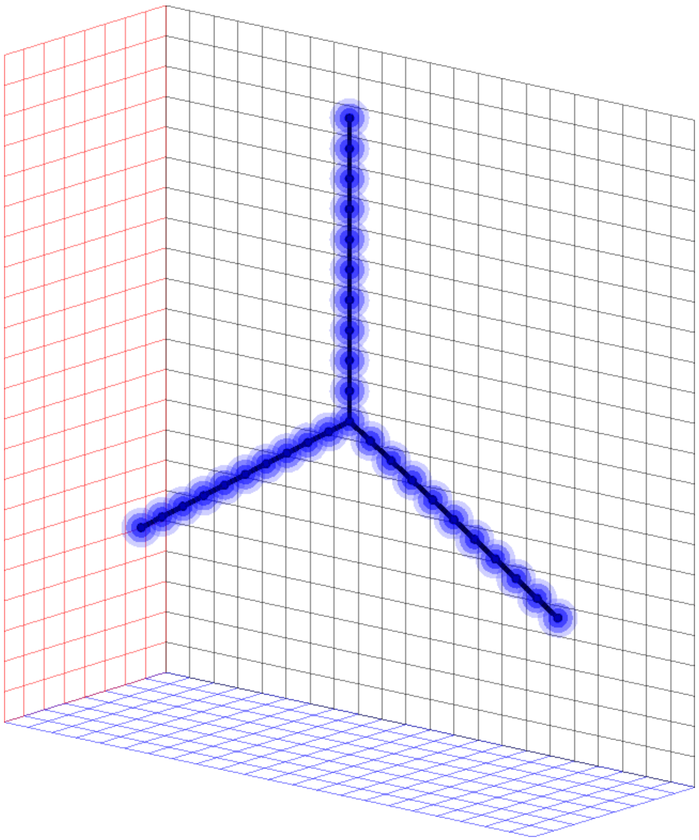

- Blades represented as lines.
- Aerodynamic blade forces determined from 2D airfoil data.
- Blade forces smeared to avoid singular behaviour.

$$\mathbf{f}_\varepsilon = \mathbf{f} \otimes \eta_\varepsilon, \quad \eta_\varepsilon = \frac{1}{\varepsilon^3 \pi^{3/2}} \exp\left[-\frac{d^2}{\varepsilon^2}\right]$$

$$\varphi = \tan^{-1}\left(\frac{V_z}{\Omega r - V_\theta}\right)$$

$$\Downarrow$$

$$\alpha = \varphi - \gamma$$

$$\mathbf{f} = \begin{pmatrix} L \\ D \end{pmatrix} = \tfrac{1}{2}\rho V_{rel}^2 c \begin{pmatrix} C_L(\alpha)\mathbf{e}_L \\ C_D(\alpha)\mathbf{e}_D \end{pmatrix}$$

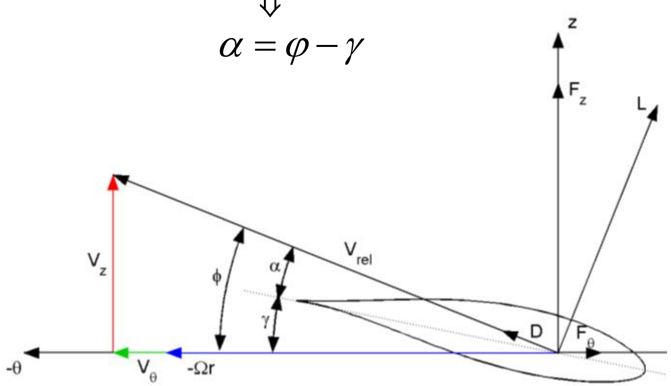


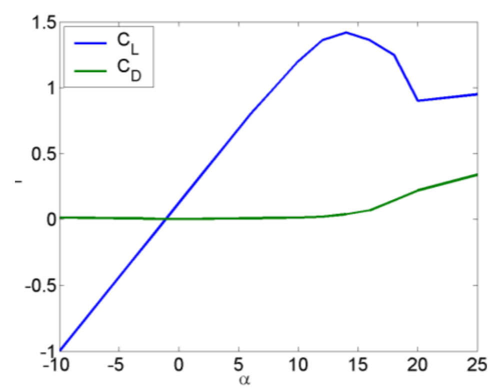

# Background

**Wind turbine models in CFD**

- Fully resolved rotor (FR)
- Actuator line model (AL)
- Actuator disc model (AD)

**Advantages:**

- Low number of grid points O($10^6$) needed compared to full rotor CFD.
- Applicable with simple grid geometries.
- Captures the most important features of the wake including tip/root vortices.
- Well suited for LES simulations (no boundary layers need to be resolved)

**Disadvantages:**

- Relies on airfoil data

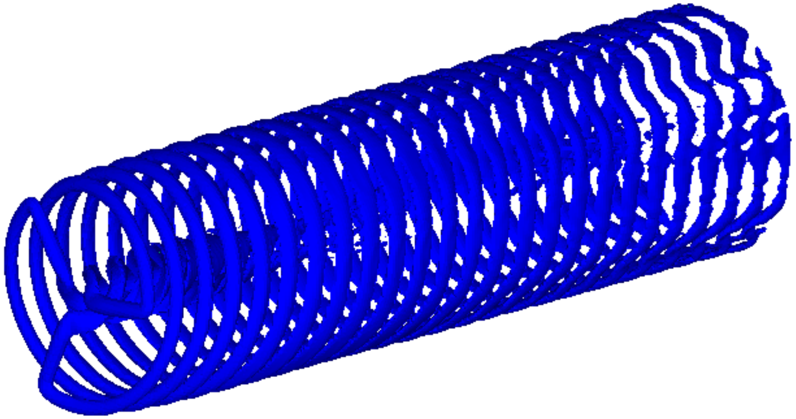

# Background

**Wind turbine models in CFD**

- Fully resolved rotor (FR)
- Actuator line model (AL)
- Actuator disc model (AD)

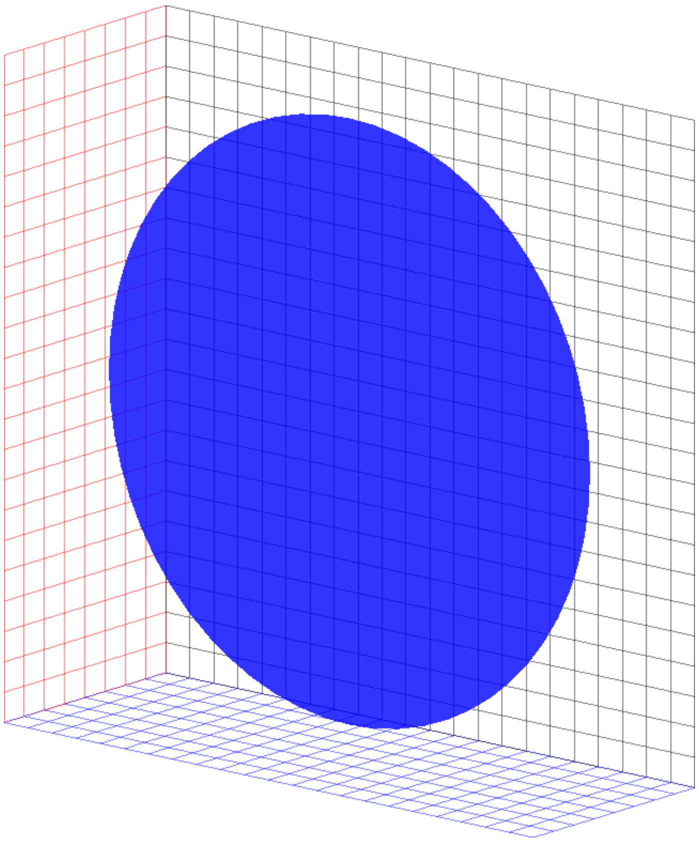

➢ Rotor represented by forces distributed on permeable disc.

# Background

**Wind turbine models in CFD**

- Fully resolved rotor (FR)
- Actuator line model (AL)
- Actuator disc model (AD)

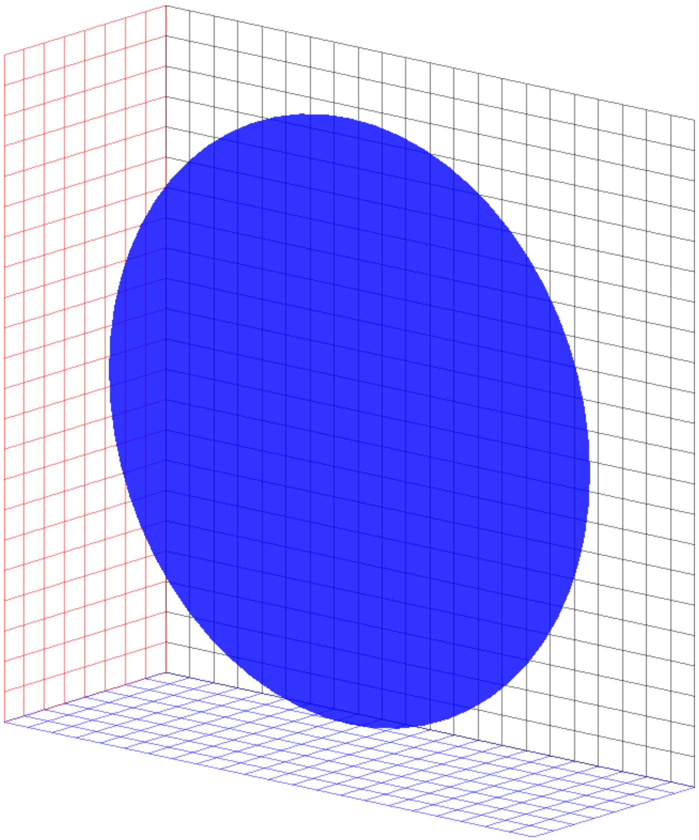

➢ Rotor represented by forces distributed on permeable disc.

➢ The disc loading is either prescribed or determined from airfoil data.

➢ Pressure velocity decoupling avoided using Gaussian force smearing or a modified Rhie-Chow algorithm

# Background

**Wind turbine models in CFD**

- Fully resolved rotor (FR)
- Actuator line model (AL)
- Actuator disc model (AD)

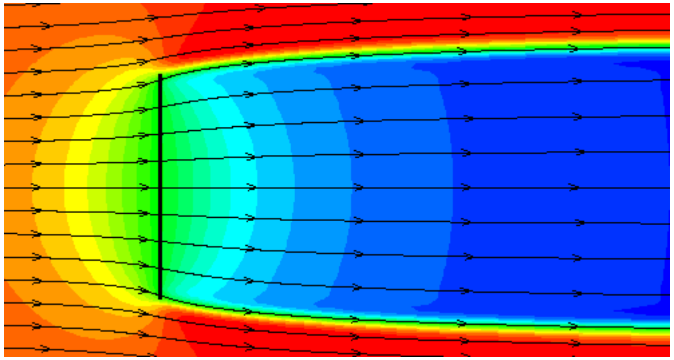

*Axial velocity contours and streamlines for a uniformly loaded disc at $C_T$=0.89*

**Advantages:**

- Low number of grid points
- Applicable with simple grid geometries
- Well suited for LES simulations
- Large time steps can be used
- Can run in steady state

**Disadvantages:**

- Relies on airfoil data
- Does not capture influence of individual blades
- May be questionable in non-uniform inflow

# Background

**Summary:**

- ➢ AL/AD typically used for wake studies
- ➢ Details of rotor geometry assumed unimportant in far wake

**Objectives:**

➢Study importance of wind turbine model on wake characteristics

- ➢ How much details are lost due to the simpler models?

- ➢ Conduct a consistent comparison of the three models
  - ➢ Same numerical setup for all models

# Previous work

**Simulations of NREL 5MW reference turbine in non-sheared laminar inflow**

- Wake of FR develops faster into a bell shaped form than the AL and AD.
- Faster spreading of wake is caused by larger TKE in the FR simulation.

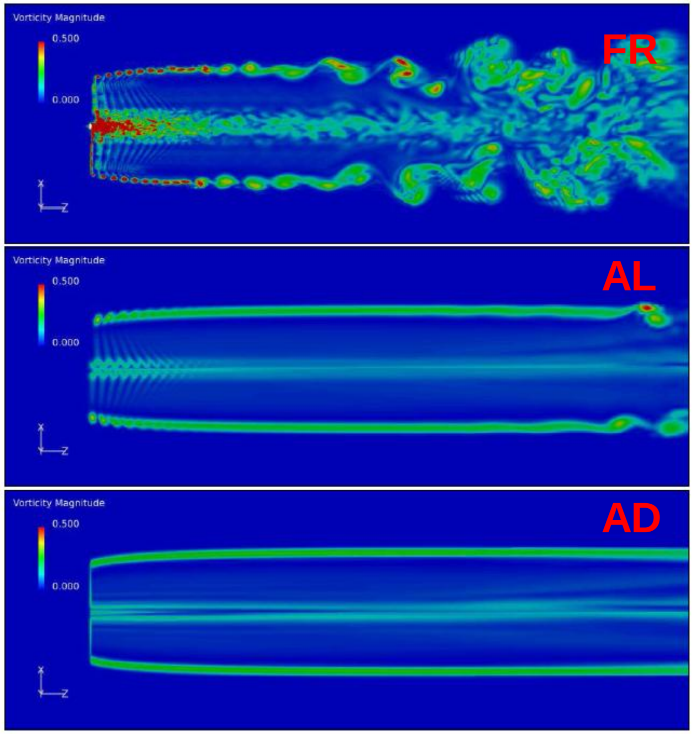


Snapshot of vorticity magnitude contours in horizontal cross-section through rotor center.

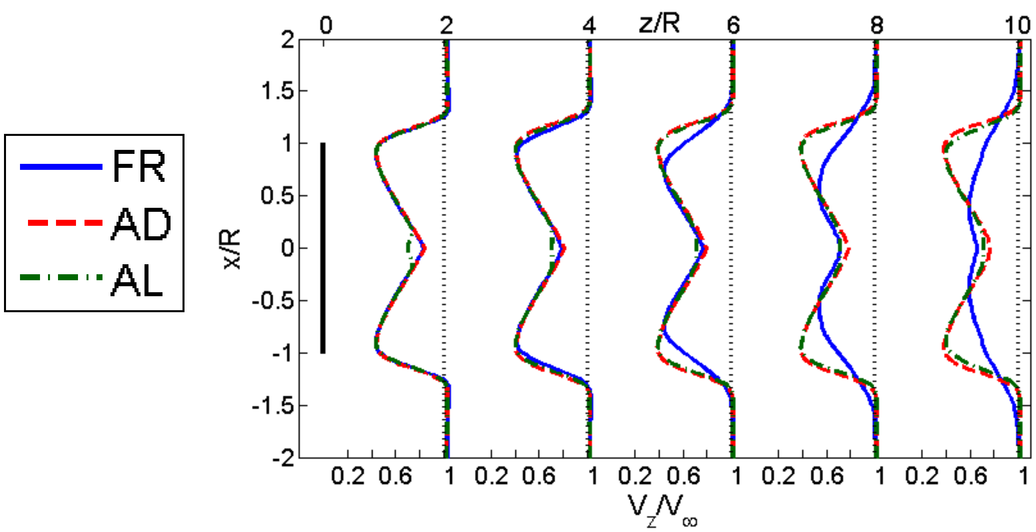


Axial velocity

# Previous work

**Simulations of NREL 5MW reference turbine in non-sheared turbulent inflow**

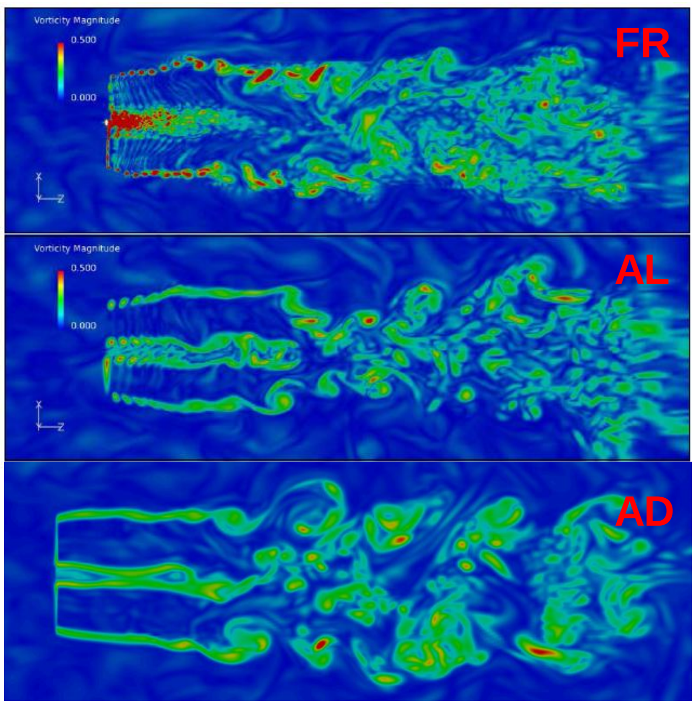


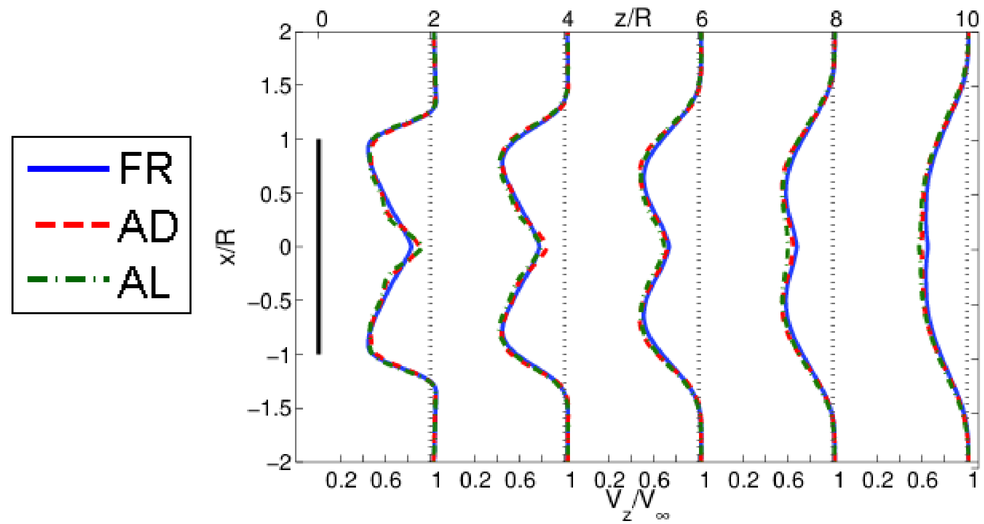


Axial velocity

Snapshot of vorticity magnitude contours in horizontal cross-section through rotor center.

# Present work

**Objectives:**

➢Study importance of wind turbine model on wake characteristics in non-uniform inflow:

- ➢ Sheared inflow
- ➢ Yawed inflow

➢ Simulating the 2MW NM80 turbine using similar numerical setup

# Approach – Flow solver

**EllipSys3D:**

- In-house CFD code
- Incompressible Navier-Stokes equations
- Finite volume discretization
- Structured curvelinear grids
- Pressure/Velocity formulation
- Multigrid
- Multiblock
- Grid sequencing
- MPI

**Solver parameters:**

- QUICK/QUICK_CDS4
- SIMPLE
- DES

# Approach - Numerical setup

**Background mesh:**

- Same background mesh for all simulations
- Half cylinder with radius 8D
- 308 blocks of $32^3$ ($10.1 \cdot 10^6$ cells)
- High resolution of the first 5D of the wake (cell size 1.3m x 1.3m x 0.8m)

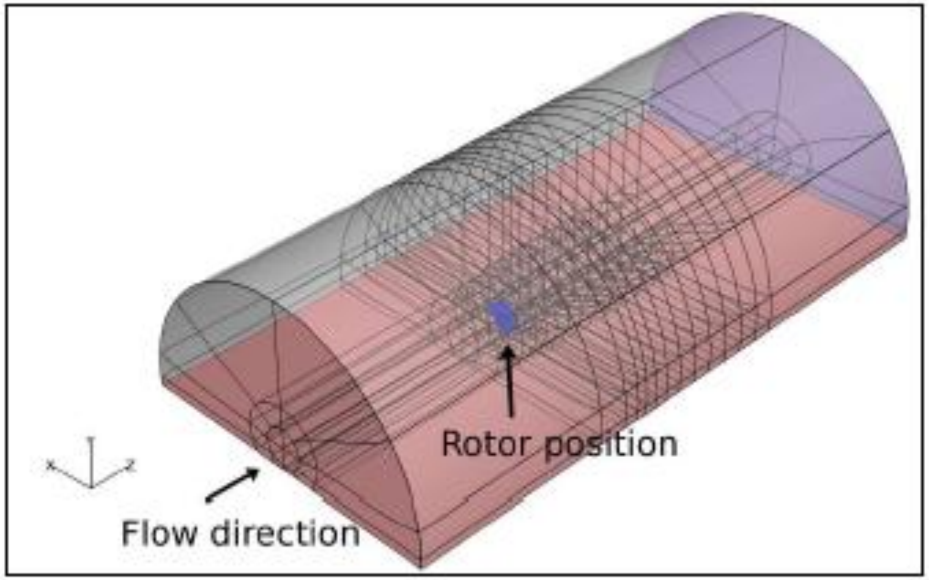

# Approach - Numerical setup

**Full rotor with overset grid:**

- Four overlapping mesh groups
- Rotor mesh generated using HypGrid3D to form an O-O topology
- Total number of grid points is $26.7\cdot10^{6}$
- Rotor surface with a non-slip boundary condition
- First cell height $y=1.0\cdot10^{6}$ ($y^{+} < 2$)

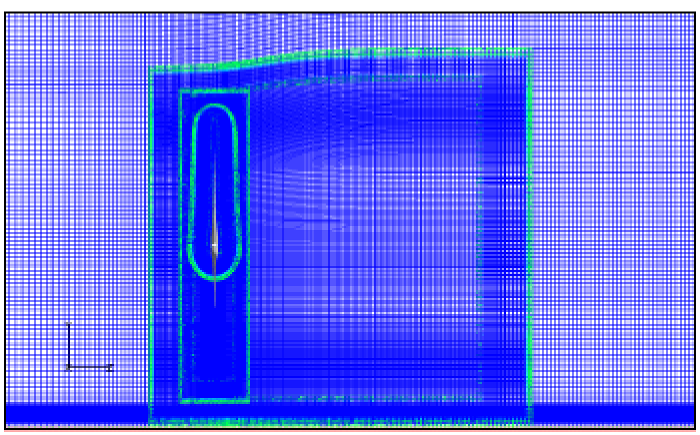

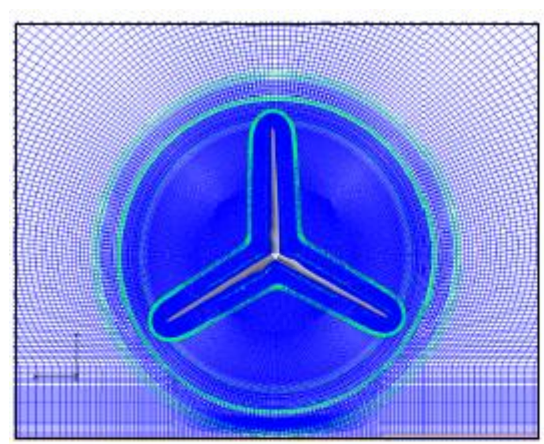

# Approach - Numerical setup

**Actuator line simulations:**

- Same background mesh as the full rotor simulation (10.1 $\cdot 10^6$ cells)
- Force smearing using 3D convolution
- 33 force elements along each line

# Approach - Numerical setup

**Actuator disc simulations:**

- Same background mesh as the full rotor simulation ($10.1 \cdot 10^6$ cells)
- 33 radial force elements
- Force smearing using 1D convolution in normal and radial direction
- Forces on each differential area dA=rdrdθ is determined from local flow conditions and airfoil data.

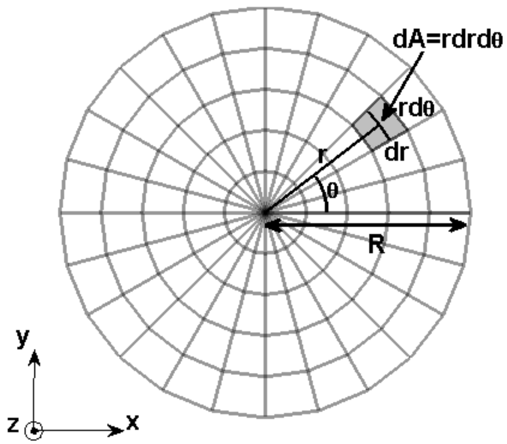


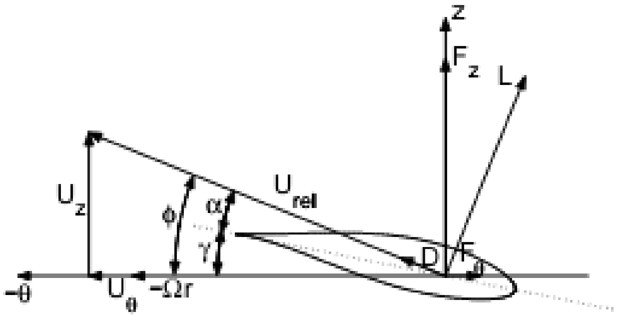

# Results

| Test cases |
| --- |
| • Sheared inflow |
| • Yawed inflow |

# Results

| Test cases |
| --- |
| • Sheared inflow |
| • Yawed inflow |

- $V_\infty$ = 8 m/s
- Power law inflow (α = 0.55):

$$V_Z = V_\infty \left( \frac{y}{H} \right)^\alpha$$

# Results

| Test cases |
| --- |
| • Sheared inflow |
| • Yawed inflow |

- Normal loads in good agreement
- Tangential loads less in FR than in AL and AD

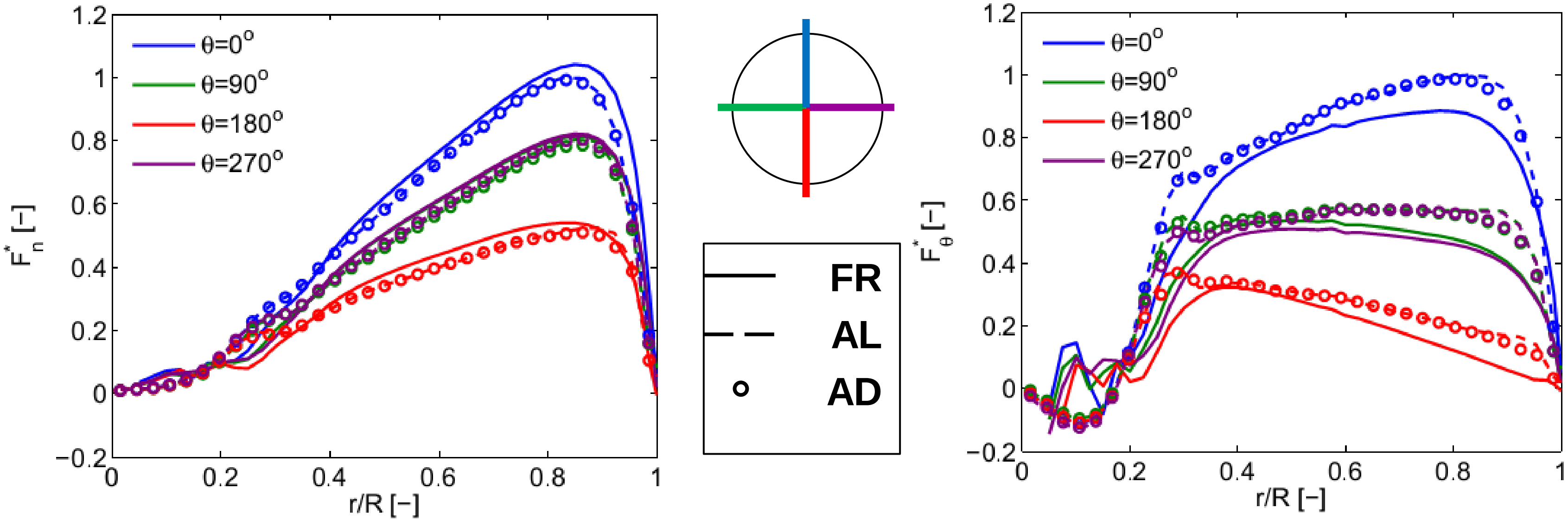


Spanwise distribution of normal and tangential loads at various azimuth positions

# Results

| Test cases |
|---|
| • Sheared inflow |
| • Yawed inflow |

- Vorticity from tip vortices much stronger in FR than in AL and AD.
- Wake of FR more unstable
- Similar vorticity contours for AL and AD (except for instabilty in the far wake)
- Reasons for more unstable wake of FR:
  - Higher grid resolution
  - Fluctuating loads (e.g. stall effets near root)

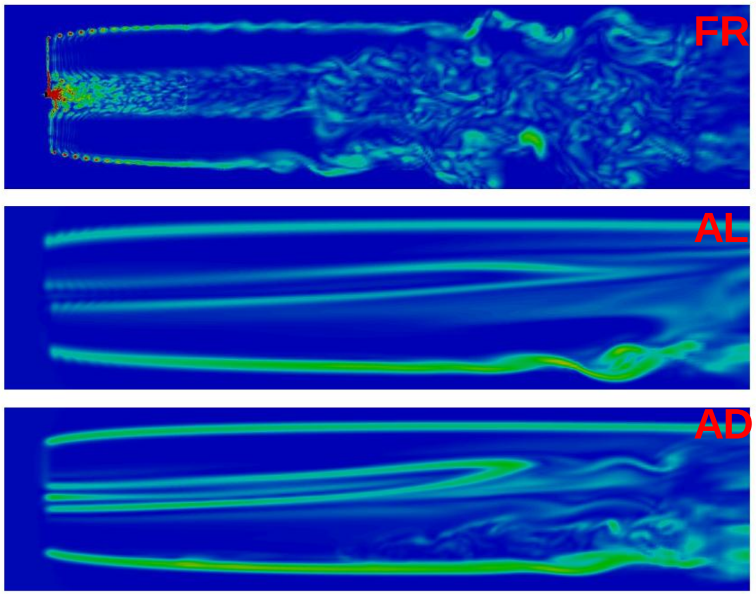


Snapshot of vorticity magnitude contours in horizontal cross-section through rotor center.

# Results

**Test cases**

- Sheared inflow
- Yawed inflow

- Good agreement in predicted near wake deficit
- AL and AD in close agreement
- Wake of FR develops faster into a bell shaped form than the AL and AD.

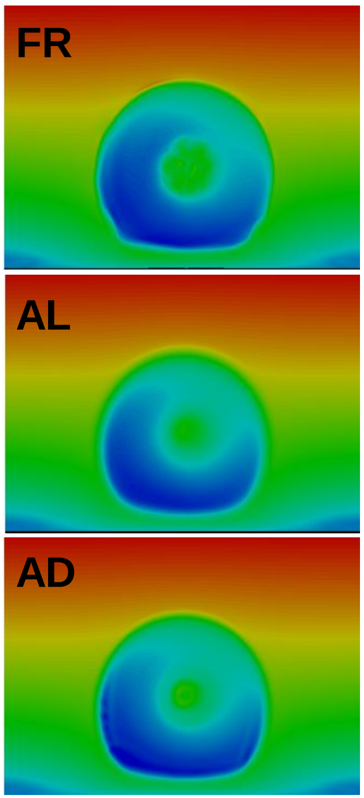


Streamwise velocity contours in cross-section 1D downstream.

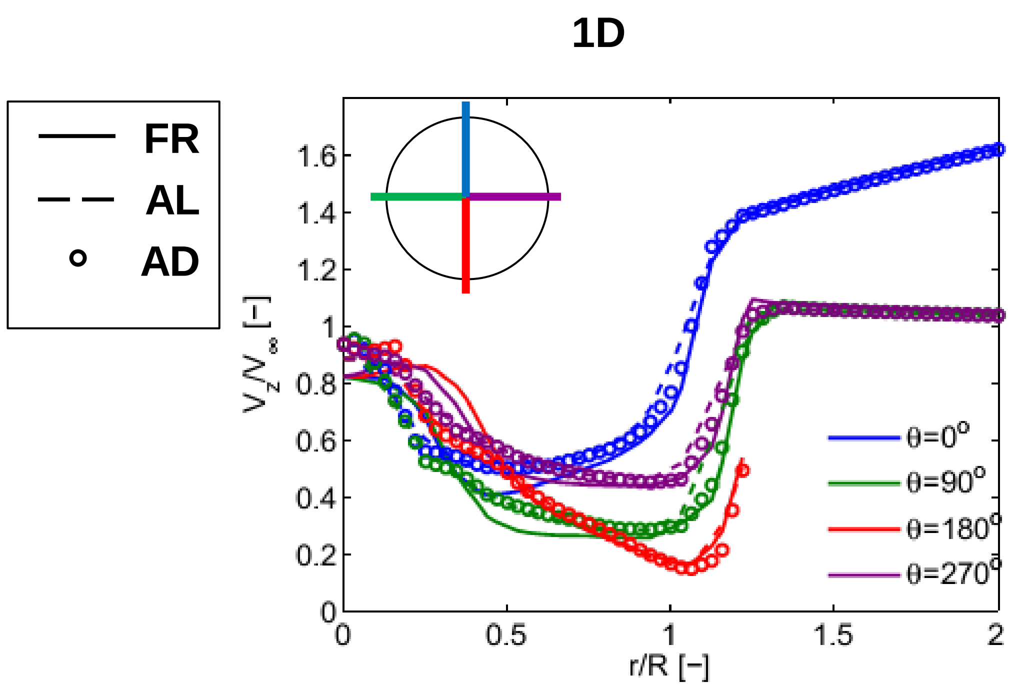


Mean streamwise velocity 1D downstream for various azimuth positions

# Results

**Test cases**
- Sheared inflow
- Yawed inflow

- Good agreement in predicted near wake deficit
- AL and AD in close agreement
- Wake of FR develops faster into a bell shaped form than the AL and AD.

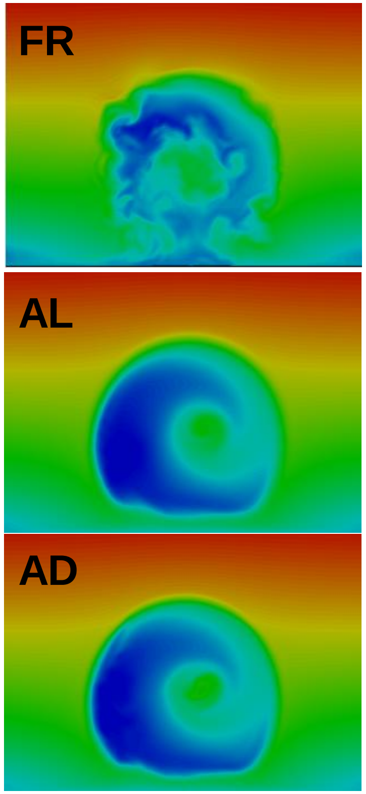


Streamwise velocity contours in cross-section 3D downstream.

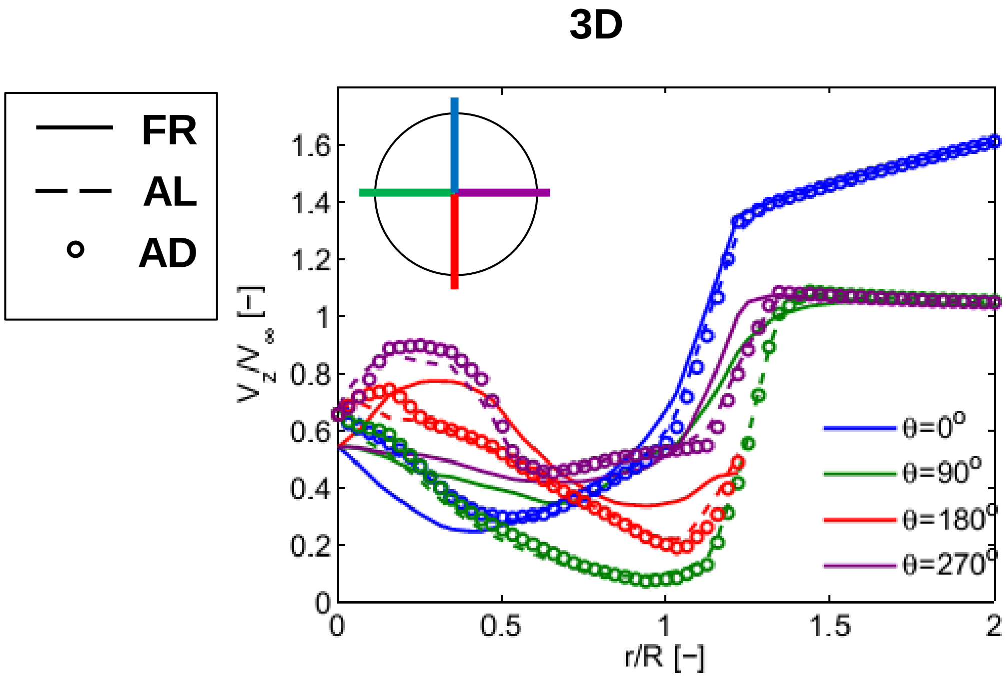


Mean streamwise velocity 3D downstream for various azimuth positions

# Results

**Test cases**

- Sheared inflow
- Yawed inflow

➢ Good agreement in predicted near wake deficit

➢ AL and AD in close agreement

➢ Wake of FR develops faster into a bell shaped form than the AL and AD.

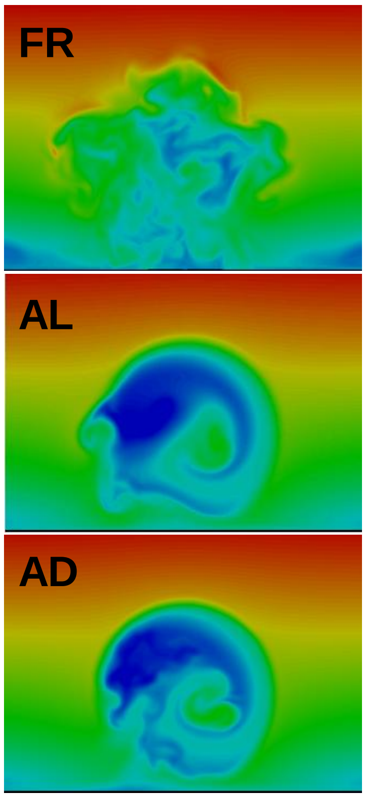


Streamwise velocity contours in cross-section 5D downstream.

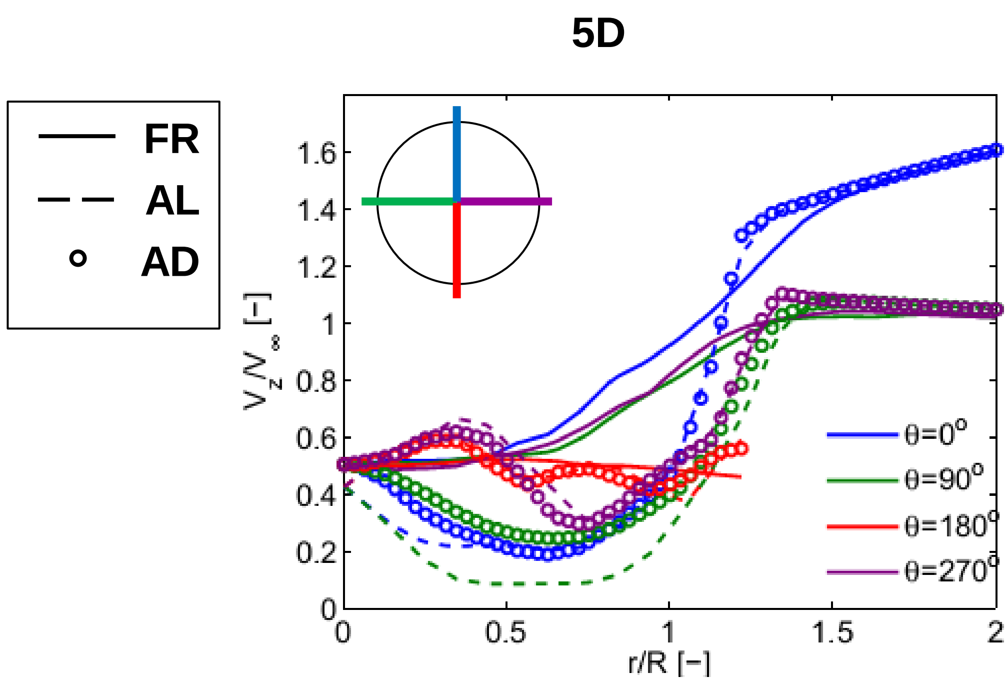


Mean streamwise velocity 5D downstream for various azimuth positions

# Results

| Test cases |
|---|
| • Sheared inflow |
| • Yawed inflow |

- $V_\infty$ = 8 m/s
- Yaw error of 20°

# Results

| Test cases |
| --- |
| • Sheared inflow |
| • Yawed inflow |

➢ Load predictions in good agreement

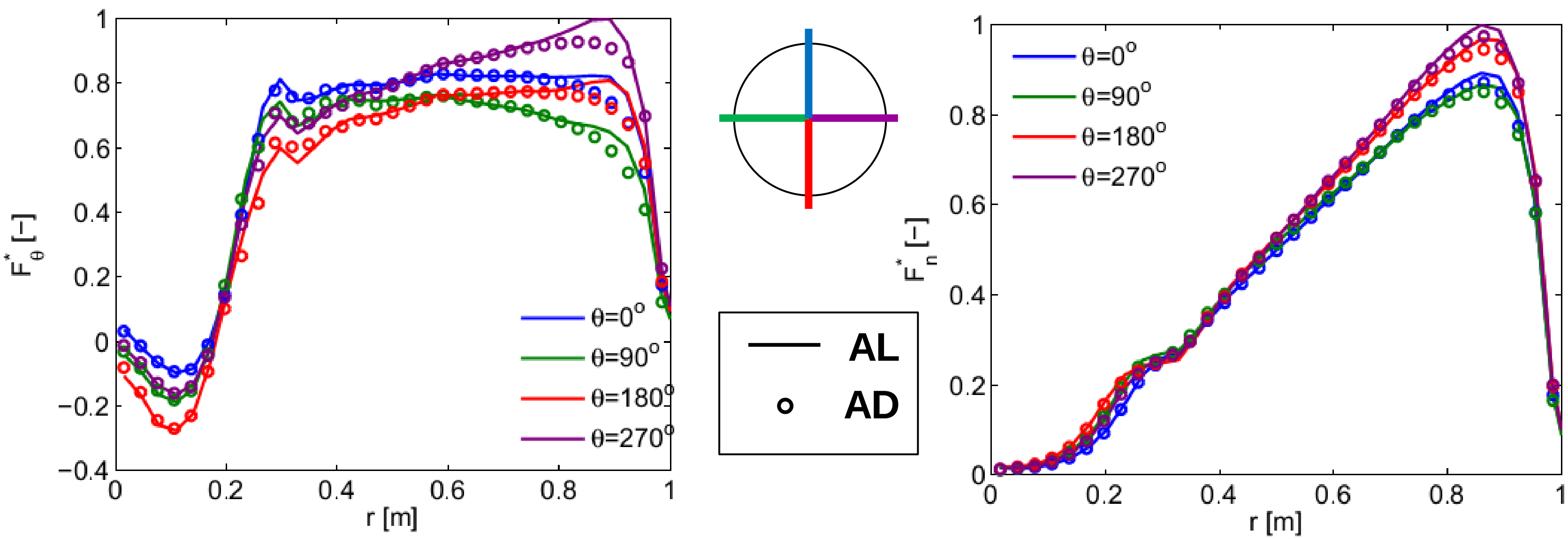


Spanwise distribution of normal and tangential loads at various azimuth positions

# Results

| Test cases |
|---|
| • Sheared inflow |
| • Yawed inflow |

➢ Similar vorticity contours

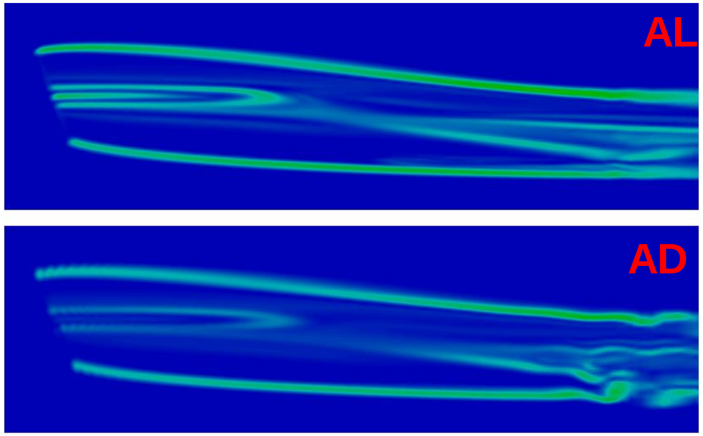


Snapshot of vorticity magnitude contours in horizontal cross-section through rotor center.

# Results

**Test cases**

- Sheared inflow
- Yawed inflow

➢ Good agreement in predicted wake deficit and wake structure

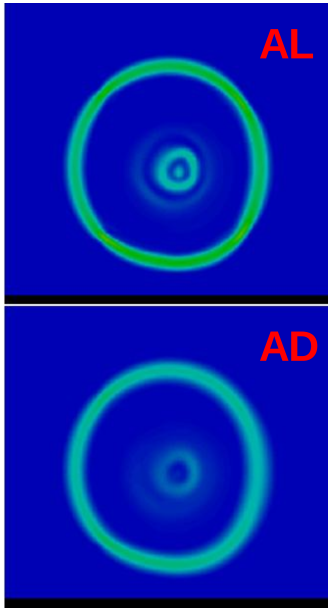


Vorticity magnitude contours in cross-section 1D downstream.

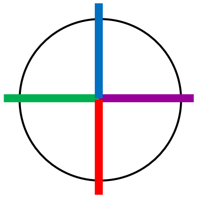

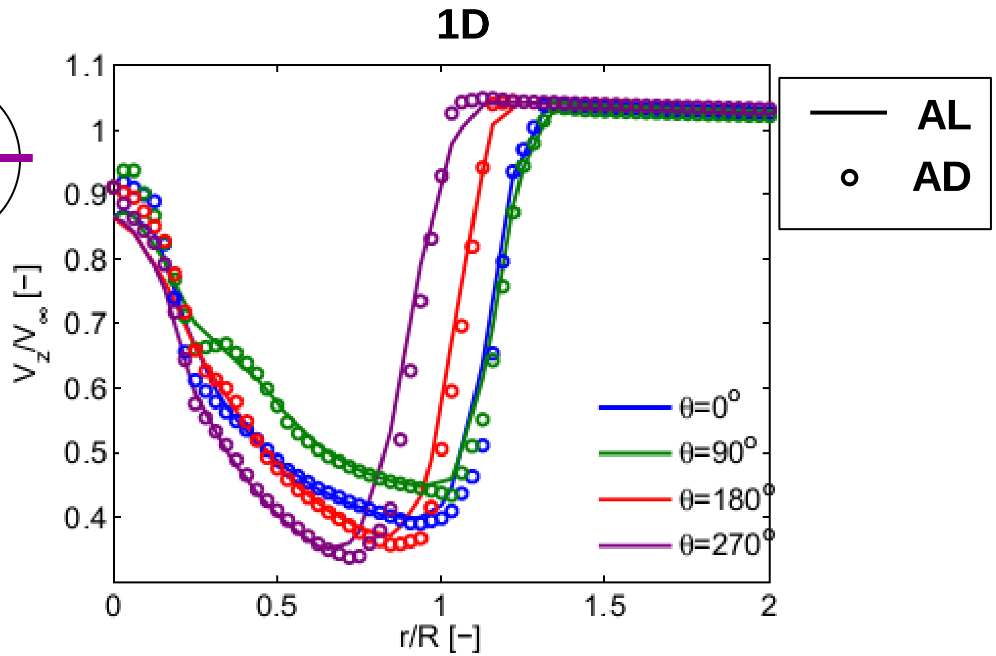


Mean streamwise velocity 1D downstream for various azimuth positions

# Results

| Test cases |
|---|
| • Sheared inflow |
| • Yawed inflow |

➢ Good agreement in predicted wake deficit and wake structure

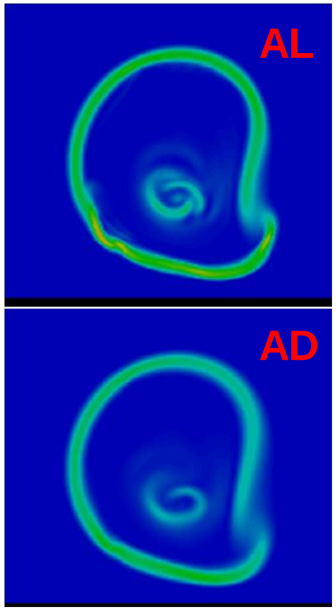


Vorticity magnitude contours in cross-section 3D downstream.

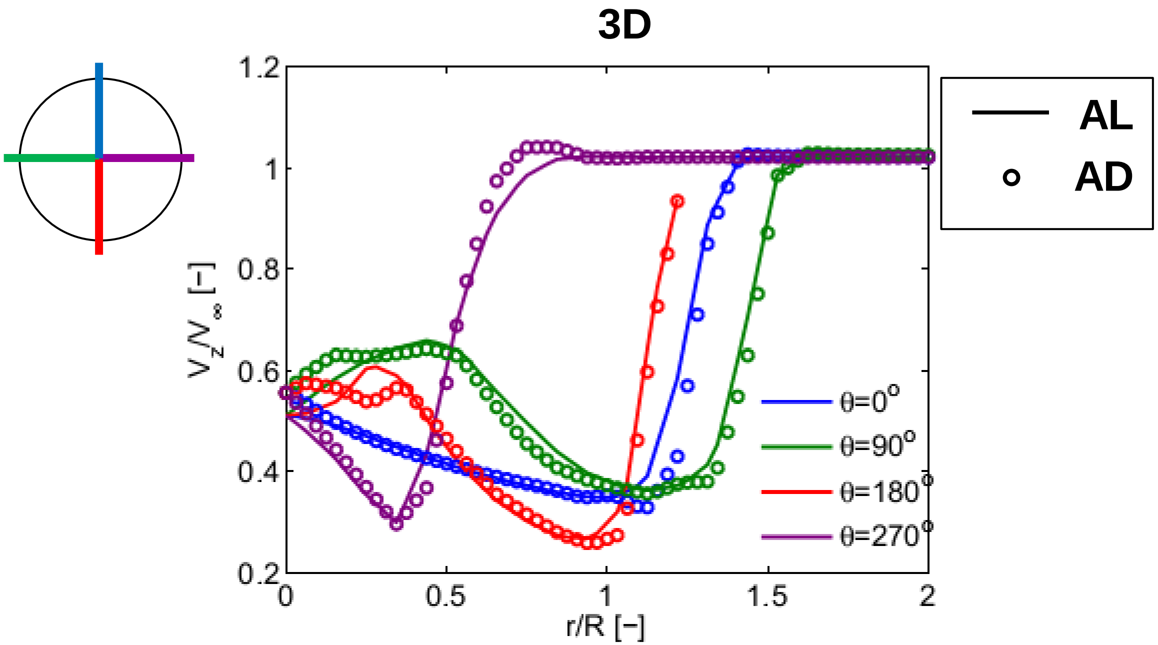


Mean streamwise velocity 3D downstream for various azimuth positions

# Results

**Test cases**

- Sheared inflow
- Yawed inflow

➢ Good agreement in predicted wake deficit and wake structure

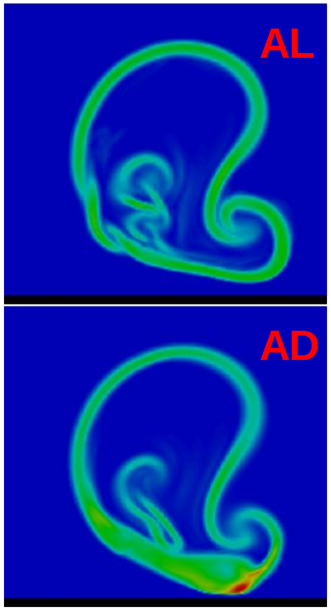


Vorticity magnitude contours in cross-section 5D downstream.

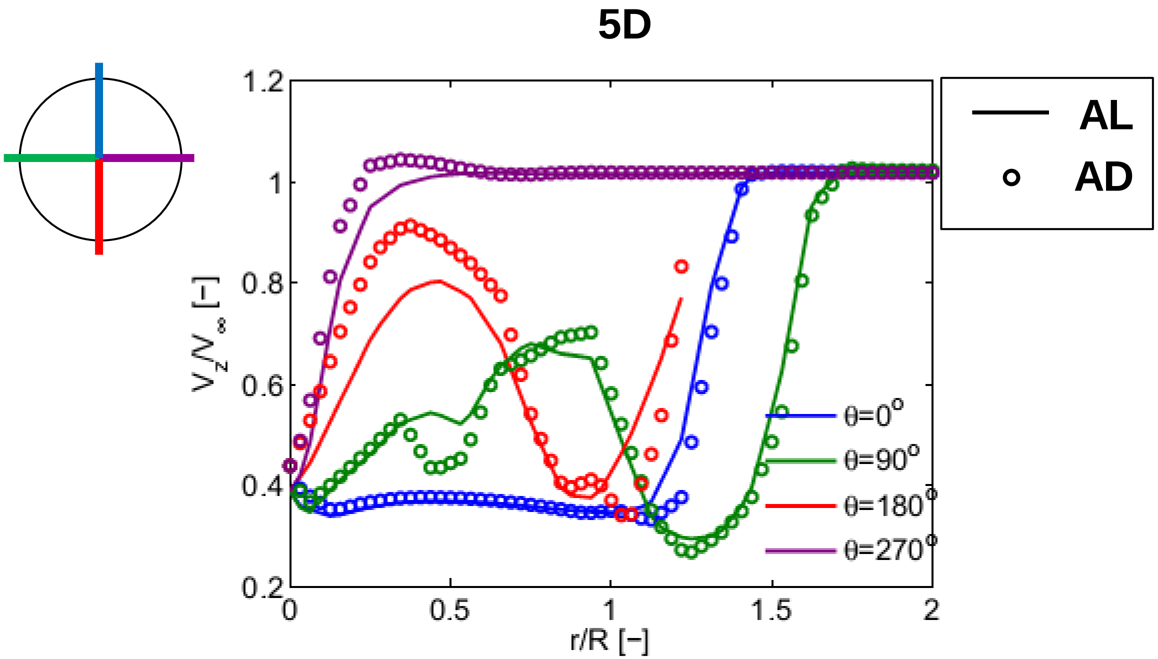


Mean streamwise velocity 5D downstream for various azimuth positions

# Conclusions

- Sheared inflow
  - Three models show good agreement in axial velocity up to 2D downstream of the turbine.
  - Further downstream the FR simulation predicts a faster smearing of the mean gradients
  - Much higher turbulence in the FR simulation
  - Generally good agreement between AL and AD for all downstream position.
- Yawed inflow
  - Good resemblance between wake behavior predicted using AL and AD.
  - AD representation as accurate as AL even in non-uniform inflow.